New Spinel Cobalt Oxides, Potential Conductive Additives for the Positive Electrode of Ni−MH Batteries

Frédéric Tronel,[†,‡] Liliane Guerlou-Demourgues,*[,†] Michel Ménétrier,[†] Laurence Croguennec,[†] Lionel Goubault,[‡] Patrick Bernard,[‡] and Claude Delmas[†]

Institut de Chimie de la Matière Condensée de Bordeaux-CNRS and Ecole Nationale Supérieure de Chimie et Physique de Bordeaux, Université Bordeaux I, 87 Avenue Dr. A. Schweitzer, 33608 Pessac Cedex, France , and SAFT−Direction de la Recherche, 111-113 Boulevard Alfred Daney, 33074 Bordeaux Cedex, France

Received January 23, 2006. Revised Manuscript Received September 13, 2006

Temperature plays a key role in the formation of the cobalt-based conductive network at the positive electrode of alkaline batteries during the first charge. Electrodes pasted with CoO were oxidized in various concentrated alkaline media, in order to understand the phenomena involved. In these conditions, the experiments show the formation of a Co_3O_4 type phase with defects. The presence of lithium in the electrolyte is proven to play an important role in the conductivity of the synthesized phases. Especially in 2.5 M LiOH, a pure phase is isolated that has a spinel structure close to Co_3O_4 but containing H and Li. This phase is shown to be a good conductor and is also observed in (KOH, NaOH, LiOH) ternary industrial electrolyte. It could hence take part to the improvement of the properties of nickel electrodes observed when the beginning of the first charge is performed at high temperature.

1. Introduction

In the field of alkaline batteries, cobalt has been much studied during the past years. For Ni−MH and Ni−Cd batteries, the positive active material is based on nickel hydroxide. Cobalt hydroxide is not a competitor to nickel as an active material, because its reversibility in energy storage is far from being as good as that of nickel hydroxide.[1] However, when added in small amounts to nickel hydroxide, cobalt has multiple positive effects on the nickel oxide electrode. When partly substituted for nickel within nickel hydroxide, it increases the difference between the active material charge potential and electrolyte oxidation potential, leading to a better chargeability and then a higher cell capacity.[2] The presence of cobalt in nickel hydroxide is also reported to increase the conductivity of nickel hydroxide[3] and prevent swelling of nickel hydroxide during cycling, especially when cadmium is cosubstituted.[4] Besides, pure cobalt derivatives can also be added to nickel hydroxide or coated on the surface of spherical nickel hydroxide particles. In this case, cobalt phases form a conducting subnetwork, connecting electronically the low conductive active material particles to the current collector. This latter use of cobalt, first proposed by Oshitani et al.,[5,6] has made manufacturing of high-capacity nonsintered nickel electrode competitive.

Pioneer work of Oshitani et al. has shown that cobalt oxy-hydroxide $HCoO_2$ was the phase constituting the conductive network.[5] Further work in our laboratory demonstrated that the conductive phase was actually a nonstoichiometric derivative of cobalt oxy-hydroxide with formula H_xCoO_2 ($x < 1$).[7] This phase was formed during the first charge of the electrode and then maintained in normal cycling conditions of the alkaline batteries. It is not reduced in current discharge conditions using a cutoff voltage in the 0.9−1 V range vs cadmium. Actually, Pralong et al. measured the thermodynamic reduction potential of $HCoO_2$ in alkaline media at 0.67 V.[8] Another key property of these cobalt derivatives consists of their ability to partly dissolve in concentrated alkaline media. A localized addition of cobalt hence results in the formation of a global conductive network through a dissolution reprecipitation process.[5,9] The more soluble CoO oxide was then often preferred to cheaper $Co(OH)_2$ as additive, because it allowed better repartition of the conductor at the surface of the nickel hydroxide particles. With CoO as starting material, the addition of a smaller amount of cobalt is therefore required to obtain the same conductivity within the nickel oxide electrode. In spite of many advantages, this technology of cobalt added electrode suffers from some

* Corresponding author. Tel: 33-5-4000-2725. Fax: 33-5-4000-6698. E-mail: guerlou@icmcb-bordeaux.cnrs.fr.
† Université Bordeaux I.
‡ SAFT−Direction de la Recherche.

(1) Benson, P.; Briggs, G. W. D.; Wynne-Jones, W. F. K. *Electrochim. Acta* **1964**, *9*, 281−288.
(2) Oliva, P.; Leonardi, J.; Laurent, J. F.; Delmas, C.; Braconnier, J. J.; Figlarz, M.; Fievet, F.; De Guibert, A. *J. Power Sources* **1982**, *8*, 229.
(3) Cressent, A.; Pralong, V.; Audemer, A.; Leriche, J. B.; Delahaye Vidal, A.; Tarascon, J. M. *Solid State Sci.* **2001**, *3* (1−2), 65−80.
(4) Oshitani, M.; Takayama, T.; Takashima, K.; Tsuji, S. *J. Appl. Electrochem.* **1986**, *16*, 403.
(5) Oshitani, M.; Yufu, H.; Takashima, K.; Tsuji, S.; Matsumaru, Y. *J. Electrochem. Soc.* **1989**, *136* (6), 1590−1593.
(6) Oshitani, M.; Watada, M.; Tanaka, T.; Iida, T. *Proc.−Electrochem. Soc.* **1994**, *303*.
(7) Butel, M.; Gautier, L.; Delmas, C. *Solid State Ionics* **1999**, *122*, 271−284.
(8) Pralong, V.; Delahaye-Vidal, A.; Beaudoin, B.; Leriche, J. B.; Tarascon, J. M. *J. Electrochem. Soc.* **2000**, *147* (4), 1306.
(9) Butel, M. Ph.D. Thesis, University of Bordeaux I, Pessac, France, 1998.

10.1021/cm060175t CCC: $33.50
Published on Web 11/15/2006

drawbacks, related to high solubility of $Co(OH)_2$ upon storage of the cell in the discharge state. Cobalt tends to move from the whole electrode to the current collector[10] or to reprecipitate, forming insulating phases like Co_3O_4.[11,12] Consequences are a loss of capacity when a battery is stored in the discharged state. Many patents have been recently proposed for new additives or processes, which could solve these problems. Proposed conducting materials are based on Na-containing phases and γ-CoOOH type phases, which are hydrated derivatives of H_xCoO_2 with a higher oxidation state for cobalt.[7,13−15] But little fundamental work is reported to explain their effect.

An industrial process used consists in beginning the first charge of Ni−MH and Ni−Cd cells at 40−80 °C, when the conductive cobalt phase is forming within the nickel oxide electrode.[16,17] In these conditions, the stability of the conducting network is significantly improved. In the electrode, a cobalt-based material, which seems to be close to the Co_3O_4 spinel phase and exhibits a good conductivity, has been identified. These results raised questions about the possible use of cobalt spinel phases as conductive additives and suggest more investigations about these phases.

Cobalt spinels have been mainly studied for their catalytic properties and as model compounds. As it is a basic, well-known phase, very few recent structural work is reported on pure Co_3O_4.[18] Holgersson et al. have already presented some characterization of substituted cobaltites.[19] More recently, a general study of possible substitution for cobalt in Co_3O_4 by other first row transition elements, or by Li, Al, Ga, Ge, and Sn, has been published by Pyke et al.,[20] showing the existence of solid solutions in all cases. In the case of nickel substitution, conductivity is improved, in comparison to Co_3O_4, according to Tareen et al.[21] Numerous works have also been carried out concerning substitution of lithium,[22−24] showing a significant improvement in the electronic conductivity. This property was mainly explained by the presence of Co^{4+} ions in octahedral sites, to ensure charge balance when lithium is substituted for Co^{2+} or Co^{3+}, thus allowing delocalization of holes in the octahedral site network and then improving conductivity.

In the present work, cobalt spinel phases were prepared by electrochemical oxidation of CoO in various alkaline media. The structure of these phases was investigated by X-ray and neutron diffraction, chemical analysis, thermogravimetric studies, and NMR measurements, and a correlation with their electronic properties was attempted.

2. Experimental Section

Material Preparation. All materials were obtained by electrooxidation of a cobalt-based electrode. The electrodes are made from a viscous paste, consisting of CoO mixed with approximately 50 wt % distilled water, which was introduced into a porous nickel foam, dried 2 h at 85 °C, and then pressed at 1 t/cm^2. No mechanical binder such as PTFE was used, considering that only one charge is performed and that the material has to be recovered from the electrodes afterward. The electrode was placed between two cadmium electrodes (with capacities much higher than that of the positive electrode), playing simultaneous roles of counterelectrode and reference electrode, with a polyamide separator to avoid a short circuit. The cell was then immersed into concentrated alkaline electrolyte. In the so-constituted Co−Cd cells, the CoO-based electrode was the positive pole and the cadmium-based electrode the negative pole. This convention will be used in the whole work, so that cell "charge" corresponds to cobalt oxidation and "discharge" to reduction. The cells were kept 4 days at room temperature after the introduction of electrolyte to complete CoO hydrolysis into $Co(OH)_2$. They were then charged at various rates. After charge, the electrodes were immersed for 24 h in distilled water, with periodic changes of the rinsing solutionto remove all trace of electrolyte. They were then dried for one night at 60 °C and milled to complete an efficient recovery of the cobalt material, which is pasted in a nickel foam. Separation of nickel, coming from the nickel foam, was performed by sieving on a sieve with 80 μm holes. The various electrolytes, charge rates, and durations used for the syntheses were (i) 8 M KOH with a charge rate of *C*/100 for 120 h, (ii) "ternary" electrolyte consisting of a mixture of LiOH, NaOH, and majority KOH (uncommunicated composition), (iii) LiOH 2.5 M, and (iv) LiOH 5 M, with a charge rate of *C*/40 for 60 h for the three last electrolytes. Electrolytes and charging rates reported in this paper are those leading to the more characteristic phases. The materials obtained in 5 M LiOH are only presented for comparison and are not completely studied.

Reference Co_3O_4 and $LiCoO_2$ phases were obtained by a classical ceramic method. Co_3O_4 was synthesized by calcination of cobalt nitrates $Co(NO_3)_2{\cdot}6H_2O$ (Fluka) at 450 °C under an oxygen flow for 15 h . A 2/3 molar ratio mixture of so-formed Co_3O_4 and Li_2CO_3 (Fluka) was heated at 850 °C for 2 days under an oxygen flow to form $LiCoO_2$. Both phases Co_3O_4 and $LiCoO_2$, thus synthesized, are considered to be ideal and stoichiometric. The latter is the so-called high-temperature form of $LiCoO_2$ (HT−$LiCoO_2$), which crystallizes in the trigonal $R\hat{m}3m$ space group.[25]

Material Characterization. X-ray diffraction (XRD) patterns were collected with a Siemens D5000 powder diffractometer equipped with a diffracted-beam monochromator (Cu Kα radiation). They were recorded with a scan step of 0.02° (2θ) for 40 s. Refinements of the crystal structure were performed using the Fullprof program with pseudo-Voigt fitting function.[26] Simulated patterns were also calculated with the same program.

(10) Pralong, V.; Delahaye Vidal, A.; Chabre, Y.; Beaudoin, B.; Tarascon, J. M. *J. Solid State Chem.* **2001**, *162* (2), 270−281.
(11) Pralong, V.; Delahaye Vidal, A.; Beaudoin, B.; Leriche, J. B.; Scoyer, J.; Tarascon, J. M. *J. Electrochem. Soc.* **2000**, *147* (6), 2096−2103.
(12) Zimmerman, A. H.; Seaver, R. *J. Electrochem. Soc.* **1990**, *137* (9), 2662−2667.
(13) Matsushita. European Patent EP 0851 516 A2, 1998.
(14) Tanaka. Japanese Patent, JP 2001−52695, 2001.
(15) Sanyo. European Patent, EP 0757 395 A1, 1997.
(16) Furukawa, D. Japanese Patent, JP330858/95, 1995.
(17) Yuasa, K. Japanese Patent, JP2003−03121.6, 2003.
(18) Tournemolle, J. N. Ph.D. Thesis, University of Paris VI, Paris, France, 1972.
(19) Holgersson, S.; Karlsson, A. *Z. Anorg. Chem.* **1929**, 384−394.
(20) Pyke, D.; Mallick, K. K.; Reynolds, R.; Bhattacharya, A. K. *J. Mater. Chem.* **1998**, *8* (4), 1095.
(21) Tareen, J. A. K.; Malecki, A.; Doumerc, J. P.; Launay, J. C.; Dordor, P.; Pouchard, M.; Hagenmuller, P. *Mater. Res. Bull.* **1984**, *19*, 989−997.
(22) Zhecheva, E.; Stoyanova, R. *Mater. Res. Bull.* **1991**, *26*, 1315.
(23) Zhecheva, E.; Stoyanova, R.; Angelov, S. *Mater. Chem. Phys.* **1990**, *25*, 351.
(24) Appandairan, N. K.; Viswanathan, B.; Gopalakrishnan, J. *J. Solid State Chem.* **1981**, *40*, 117.
(25) Gummow, R. J.; Liles, D. C.; Thackeray, M. M. *Mater. Res. Bull.* **1993**, *28*, 235.
(26) Rodriguez-Carvajal, R. In *Proceedings of the Satellite Meeting on Powder Diffraction of the XV Congress of the IUCr*, Toulouse, France, July 16−18, 1990; p 127.

The neutron diffraction diagrams were recorded at Institut Laue Langevin in Grenoble (France) on the high-resolution D2B diffractometer, at room temperature, with a scan step of 0.05° between 0 and 162° (2θ). The samples were placed in a vanadium cylindrical sample holder, with a diameter of 8 mm and a height of 5 cm. As for X-ray, the refinement of the neutron data was performed with the Fullprof program.

Determination of cobalt amount was performed by EDTA complexometric titration. Inductively coupled plasma (ICP) was used for Li, Na, K, and Ni titration, and elementary organic microanalysis was used for C and H titration; both techniques were performed at the CNRS facility in Vernaison (France).

The oxidation state of cobalt was determined by the iodometric titration method. Cobalt at an oxidation state higher than two in the sample is reduced by I^- into Co^{2+}, whereas I^- is oxidized into I^0 (forming I_2). Back-titration of I_2 by $Na_2S_2O_3$ (0.1 M) allows the average oxidation state of cobalt to be deduced. The studied samples were especially hard to dissolve in the reducing medium. Around 50 mg of the sample was introduced with a KI/hydrochloric acid solution (10 mL of 10 g/L of KI, 10 mL of 6 M HCl) in a PTFE made airtight container. The same volume of solutions without powder was introduced into a second container constituting a reference sample. Both containers were placed at 60 °C for 15 h to perform s complete reduction of the sample. Such a method is better for avoiding I_2 evaporation at high temperature; back-titration is performed after complete cooling of the sample. The titrated volume of the reference sample was then subtracted in order to take dissolved oxygen into account.

Thermogravimetric analysis (TGA), coupled with mass spectroscopy (MS), was performed under an argon flux at a rate of 3 °C/min, from room temperature to 950 °C.

^{7}Li MAS NMR spectra were recorded on a Bruker Avance 300 spectrometer at 116.6 MHz, using a standard 4-mm Bruker MAS probe with a 15 kHz spinning speed. A Hahn echo sequence was used with 2.4 μs 90° pulse. The interpulse delay was equal to one rotor period (66.67 μs). The recycling time between two scans was 2 s. The reference used (0 ppm) was 1 M LiCl in aqueous solution. The samples were mixed with 50 wt % dry silica to facilitate spinning and improve the field homogeneity.

Electronic conductivity measurements were performed with the four-probe technique,[27] using a direct current in the 170−370 K temperature range. The temperature was decreased to 170 K and then progressively raised to 370 K. Because of their low-temperature synthesis, these materials could not be sintered. The pellets (8 mm in diameter and approximately 1.2 mm in thickness) were obtained by compacting around 200 mg of powder at 8 t/cm^2 under vacuum.

For thermoelectric measurements, similar pellets were used but containing 100 mg of powder, pressed at 8 t/cm^2 and with a diameter of 5 mm (approximate thickness of 1.5 mm). Measurements were recorded with a homemade apparatus.[28]

3. Structural Characterization

Preliminary work has shown that the nature of the material obtained at the end of the electro-oxidation process and its electronic conductivity are very sensitive to the electrolyte composition. The three studied samples, the synthesis method of which is described more precisely in the experimental section, will be denoted, in the following, as Co_3O_4 (8 M KOH), Co_3O_4 (ternary), and Co_3O_4 (2.5 M LiOH). In the present paper, we focused on the structural features of the materials recovered after the oxidation and on the relationship with conductive properties. The oxidation mechanism will be discussed in a forthcoming paper.

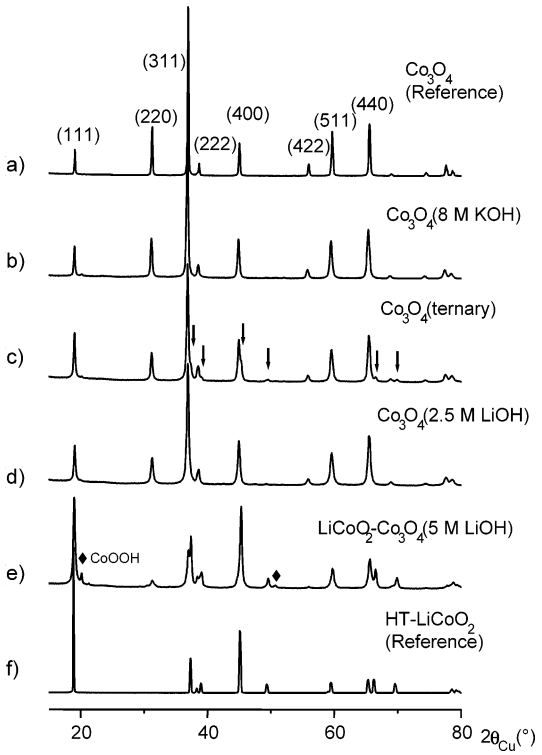

Figure 1. Comparison of the XRD patterns of (a) a reference Co_3O_4 sample with the three studied samples (b) Co_3O_4 (8 M KOH), (c) Co_3O_4 (ternary) (↓ = position of $LiCoO_2$ impurity peaks), (d) Co_3O_4(2.5 M LiOH), and two other reference samples (e) $LiCoO_2-Co_3O_4$ (5 M LiOH) obtained by the same electrochemical process (◆ = position of CoOOH impurity peaks), (d) Co_3O_4 (2.5 M LiOH), and (f) reference HT−$LiCoO_2$ phase.

XRD Features of the Obtained Materials. The XRD patterns of the three obtained materials are displayed in Figure 1b−d. Three other XRD patterns are also presented as references: pure Co_3O_4 (Figure 1a), pure HT−$LiCoO_2$ (Figure 1f), and a sample containing a mixture of $LiCoO_2$ (majority) and Co_3O_4 obtained by a similar process as the studied samples but in 5 M LiOH (Figure 1e). This latter material will be denoted as $LiCoO_2-Co_3O_4$ (5 M LiOH). In that case, a small amount of CoOOH is also present as an impurity (designated by ◆ in Figure 1). The three studied materials seem to exhibit a structure close to that of Co_3O_4: the general shape of the patterns is the same and no significant shift of the peaks is observed. However, some changes are noticeable. On one hand, in the case of Co_3O_4 (ternary) and Co_3O_4 (2.5 M LiOH), the intensity ratio of the first two peaks, indexed as (111) and (220) in the cubic system, is opposite to that observed for Co_3O_4 (8 M KOH) or for reference Co_3O_4. On the other hand, some impurity peaks appear clearly in the pattern of Co_3O_4 (ternary). At first sight, these peaks seem to correspond to $LiCoO_2$ (Figure 1f). Such a phase could be expected in an electrolyte containing lithium. Actually, several authors have already reported the synthesis of $LiCoO_2$ at low temperature in a

(27) Laplume, J. In *L'onde électrique*; **1955**, *335*, 113−125.
(28) Dordor, P.; Marquestaut, E.; Villeneuve, G. *Rev. Phys. Appl.* **1980**, *15*, 1607−1612.

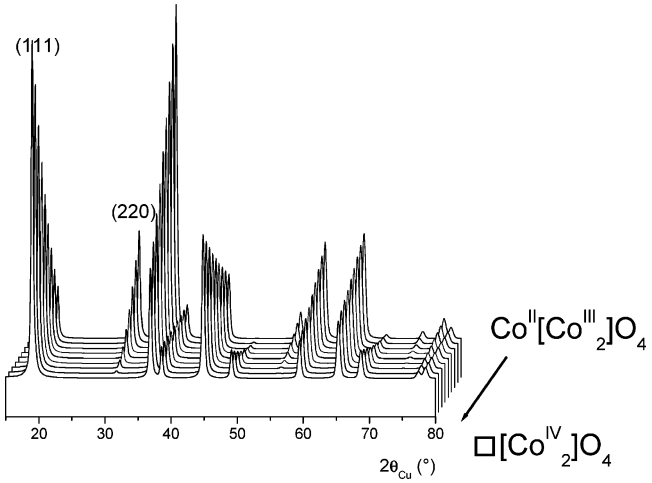

Figure 2. Simulated XRD patterns, showing the evolution of the XRD pattern of the spinel phase $Co[Co_2]O_4$ (Co_3O_4) when an increasing number of vacancies are created in the tetrahedral sites, up to the theoretical composition $\square[Co_2]O_4$.

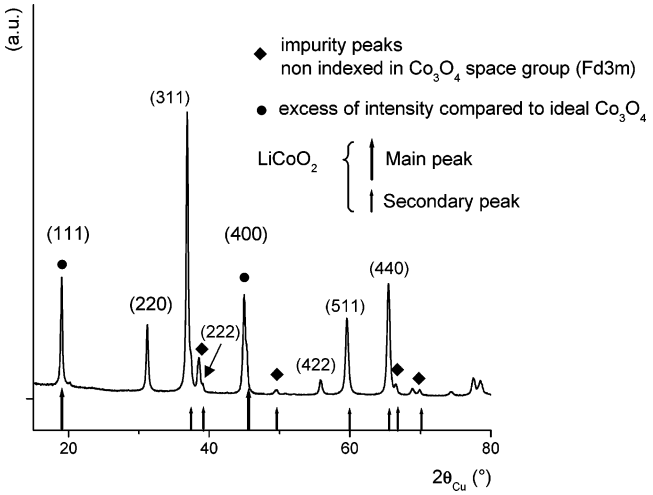

Figure 3. XRD pattern of Co_3O_4(ternary) showing the differences in line intensity with ideal Co_3O_4. Positions of $LiCoO_2$ major peaks are displayed, showing that anomalies could come from a significant amount of that latter phase in the sample.

LiOH medium.[29,30] But surprisingly, there is no trace of similar peaks for Co_3O_4 (2.5 M LiOH). It should be noticed that the amount of this impurity varies from one synthesis trial to another in ternary electrolyte. In some samples obtained in 2.5 M LiOH, $LiCoO_2$ impurity can also be observed, but the corresponding lines are always less intense than for the ternary electrolyte. Two hypotheses were examined to explain these anomalies, which will be presented in the next paragraphs.

On the one hand, cobalt vacancies in the spinel structure can be considered in order to explain the variation in intensity of the first two diffraction lines. The Co_3O_4 structure can be described as being a subnetwork of Co^{3+} in octahedral edge-sharing sites. Co^{2+} ions are located in tetrahedral sites inserted in the channels formed by the octahedral network and sharing only corners with octahedra. Considering the two types of sites for cobalt, two types of vacancies can be considered. XRD patterns were simulated considering both types of vacancies. In Figure 2, the expected evolution of the diffraction pattern starting from ideal Co_3O_4 and creating vacancies in the Co^{2+} sites up to 100%, leading to the theoretical formula $(Co)_2O_4$, is presented. It is noticeable that, when a certain number of cobalt vacancies are present in tetrahedral sites, the resulting pattern exhibits the anomalous (111)/(220) peak inversion ratio observed with Co_3O_4 (2.5 M LiOH) and Co_3O_4 (ternary). Similar simulations were performed for vacancies in octahedral sites, but the evolution of the pattern (not presented), showing especially a decrease of the (111)/(220) peak ratio, was not in good agreement with that observed for the studied samples.

On the other hand, the effect on the pattern of a significant amount of $LiCoO_2$ mixed with Co_3O_4 in the sample was investigated. For Co_3O_4 (ternary), we already mentioned some small impurity peaks corresponding to the $LiCoO_2$ phase. Figure 3 is a more detailed view of Figure 1c, shown in order to illustrate this point. Considering the position of the observed impurity peaks, attributed to the $LiCoO_2$ phase, they are not the most intense diffraction lines but secondary diffraction lines for that phase. Actually, the two main diffraction lines of $LiCoO_2$ are located at the same position as the (111) and (400) diffraction lines of Co_3O_4. Moreover, these two peaks show an excess of intensity compared to ideal Co_3O_4 (panels a and c of Figure 1). Therefore, the anomalies could also be related to significant presence of $LiCoO_2$, which is difficult to observe with XRD. Because $LiCoO_2$ is known as a good electronic conductor as soon as lithium is partly deintercalated,[31] the good conductivity of some of the studied samples could hence be explained by the presence of this latter phase.

The above general analysis of the different diffraction patterns obtained does not allow us to conclude unambiguously the formation of Co_3O_4 type phases with cobalt vacancies in tetrahedral sites or an ideal Co_3O_4 phase mixed with a significant amount of secondary $LiCoO_2$ phase. X-ray and neutron data refinements for the various materials are presented below.

X-ray and Neutron Data Refinements. Diffraction data refinements were performed on both X-ray and neutron diffraction patterns for Co_3O_4 (ternary), Co_3O_4 (2.5 M LiOH) and Co_3O_4 (8 M KOH), in order to extract more information about the presence of $LiCoO_2$ and cobalt vacancies.

Hypotheses. The refinement of the XRD and neutron data was performed considering a spinel structure for the Co_3O_4 type phase (*Fd*3*m* cubic space group). In this structure, Co ions are located in the tetrahedral 8a sites (1/8, 1/8, 1/8) and in the octahedral 16d sites (1/2, 1/2, 1/2), O is located in the 32e ((*x*, *x*, *x*) with $x \approx 0.25$) sites. Cell parameters, parameters of the pseudo-Voigt profile function, position of oxygen, cobalt occupancies in both sites (8a and 16d), and atomic displacement parameters (B_{iso}) for the three sites were refined for the spinel phase in each sample. The presence of a $LiCoO_2$ secondary phase has been considered

(29) Amatucci, G. G.; Tarascon, J. M.; Larcher, D.; Klein, L. C. *Solid State Ionics* **1996**, *84*, 169−180.
(30) Han, K. S.; Song, S.-W.; Yoshimura, M. *J. Am. Ceram. Soc.* **1998**, *81* (9), 2465−68.
(31) Ménétrier, M.; Saadoune, I.; Levasseur, S.; Delmas, C. *J. Mater. Chem.* **1999**, *9*, 1135.

Table 1. Parameters and Reliability Factors Obtained by the Rietveld Refinement of the Neutron Diffraction Pattern of the Co_3O_4 (2.5 M LiOH) Material[a]

atom	site	Wyckoff positions			occupancy	B (Å^2)
		Co_3O_4 Type Phase, Space Group $Fd3m$, a_{cub} = 8.0706 (3) Å				
Co	8a	0.125	0.125	0.125	0.64 (4)	0.6 (3)
Co	16d	0.5	0.5	0.5	0.92 (2)	0.3 (1)
O	32e	0.2625 (5)	0.2625 (5)	0.2625 (5)	1	0.71 (4)
		$LiCoO_2$ Type Phase, Space Group $R\bar{3}m$, a_{hex} = 2.82 Å, c_{hex} = 14.01 Å				
Li	3b	0	0	0.5	1	1.2
Co	3a	0	0	0	1	0.5
O	6c	0	0	0.26	1	0.8
		CoO Type Phase, Space Group $Fm3m$, a_{cub} = 4.279 (7) Å				
Co	4a	0	0	0	1	0.5
O	4b	0.5	0.5	0.5	1	0.8
		Ni Type Phase, Space Group $Fm3m$, a_{cub} = 3.523 (2) Å				
Ni	4a	0	0	0	1	0.5

Conditions of the Run	
T (K)	300
angular range	$10° \le 2\theta \le 162°$
step scan increment (2θ)	0.05°
zero point (2θ)	0.042 (3)°
no. of fitted params	24

Profile Params			
pseudo-Voigt function	PV = ηL + (1 − η)G	η = 0.61 (5)	
half-width params	U = 0.33 (2)	V = −0.06 (4)	W = 0.14 (1)

Composition (%)	
Co_3O_4	97
$LiCoO_2$	0.5
CoO	1.1
Ni	1.4

Conventional Rietveld R-factors for points with Bragg contribution (%)			
R_{wp}	10.4	$R_{B_{Co3O4}}$	3.7
$R_{B_{LiCoO2}}$	12.2	$R_{B_{CoO}}$	5.5
$R_{B_{Ni}}$	21.6		

[a] Standard deviations have been multiplied by the Scor number (2.7) to correct local correlations.

for Co_3O_4 (ternary) and Co_3O_4 (2.5 M LiOH). The structure of $LiCoO_2$ was described in the $R\bar{3}m$ trigonal space group, corresponding to the HT−$LiCoO_2$ form. Only the a_{hex} and c_{hex} cell parameters were refined for $LiCoO_2$, the atomic positions were fixed to values reported in literature.[32] Indeed, because of the presence of $LiCoO_2$ in small amounts, the refinement of all its structural parameters was not possible. For the same reason, the profile function that describes its diffraction lines was constrained to be the same as the one used for the Co_3O_4 type phase. When their presence was noticeable on the collected pattern, impurities such as CoO, metallic nickel, and CoOOH were taken into account, though the refinements always estimated their amounts as being less than 2 wt %. As for $LiCoO_2$, the same profile function was used and only the cell parameters were refined.

Results. The results of the refinement of the neutron diffraction pattern of the Co_3O_4 (2.5 M LiOH) material are presented in detail in Table 1. This material is indeed very interesting because it is constituted for the major part of a spinel phase, with a negligible amount of $LiCoO_2$. A comparison between the experimental and calculated neutron diffraction patterns is shown in Figure 4. As mentioned above, small amounts of CoO and Ni were considered in addition to Co_3O_4 and $LiCoO_2$ for this refinement. All the refinement results (XRD and neutron) of the different samples are compared in Table 2. The quality of the refinements was generally quite good according to the quality factors, and no important deviation could be seen on the patterns.

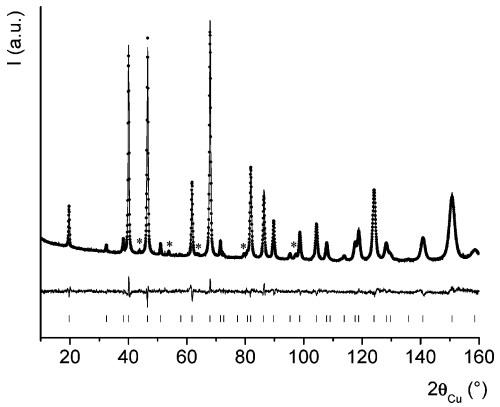

Figure 4. Comparison of the experimental (●) and calculated (−) neutron diffraction patterns for the Co_3O_4 (2.5 M LiOH) phase. The diagrams were replotted vs $2\theta_{Cu}$. The difference ($I_{obsd} - I_{calcd}$) and the positions of the diffraction lines are also given (|). (* = peaks of the secondary phases)

Concerning the spinel phase, refinements show unambiguous cobalt vacancies: cobalt occupancies are in the range {0.64−0.88} in tetrahedral sites (8a), and {0.90−0.95} in octahedral sites (16d), instead of one in each site for the ideal Co_3O_4. The number of vacancies in tetrahedral sites seems to slightly increase from Co_3O_4 (8 M KOH) to Co_3O_4 (ternary); the larger amount is obtained for Co_3O_4 (2.5 M

(32) Levasseur, S.; Ménétrier, M.; Suard, E.; Delmas, C. *Solid State Ionics* **2000**, *128*, 11.

Table 2. Comparison of the Main Crystallographic Parameters for Co_3O_4 (2.5 M LiOH), Co_3O_4 (ternary), and Co_3O_4 (8 M KOH) Obtained by Rietveld Refinements of X-ray and Neutron Diffraction Patterns[a]

	Co_3O_4 (8 M KOH)		Co_3O_4 (ternary)		Co_3O_4 (2.5M LiOH)	
	X-ray	neutron	X-ray	neutron	X-ray	neutron
	Spinel Phase "Co_3O_4" Type, Space Group *Fd3m*					
a (Å)	8.1006 (7)	8.0934 (5)	8.0803 (7)	8.0807 (3)	8.0741 (9)	8.0706 (3)
Co occupancy 8a site (%) (tetrahedral)	0.88 (2)	0.78 (7)	0.81 (2)	0.77 (4)	0.73 (1)	0.64 (4)
Co occupancy 16d site (%) (octahedral)	0.94 (2)	0.95 (3)	0.93 (2)	0.91 (2)	0.90 (2)	0.92 (2)
R_B (%)	3.7	5.6	2.6	4.3	3.6	3.7
	$LiCoO_2$ Phase, Space Group $R\bar{3}m$					
a_{hex} (Å)			2.8186 (6)	2.8168 (4)		2.82
c_{hex} (Å)			14.036 (5)	14.064 (5)		14.01
R_B (%)			6.4	8.3		12.2
% $LiCoO_2$	0	0	19.5	19.1	0	0.5
R_{wp}	17.2	13.4	14.7	12.4	15	10.4

[a] In the case of the lithium-containing sample, the evaluated amount of $LiCoO_2$ secondary phase is also reported.

Table 3. Weight Percentages of Different Elements, Molar Ratios, and Average Cobalt Oxidation State for the Studied Samples Co_3O_4 (2.5 M LiOH), Co_3O_4 (ternary) and Co_3O_4 (8 M KOH) and for References

	wt %									
sample	Co	Li	Na	K	H	Li/Co	Na/Co	K/Co	H/Co	average cobalt oxidation state
Co_3O_4 (ternary)	68.6	1.3	380 ppm	0.15	0.27	0.17	0.001	0.003	0.23	2.75
Co_3O_4 (2.5M LiOH)	70.2	0.6	75 ppm	40 ppm	0.27	0.073	4×10^{-4}	8×10^{-5}	0.23	2.72
Co_3O_4 (8 M KOH)	70.5	0	0	0.55	0.31	0	0	0.012	0.26	2.68
Co_3O_4 (theoretical)	73.4	0								2.66
$LiCoO_2$ (theoretical)	60.2	7.1				1				3
$Co_{2.6}O_4$ (theoretical)	70.5	0								3.07

LiOH). In all cases, the amount of vacancies in the tetrahedral site obtained from the neutron data is larger than that obtained from the X-ray diffraction data. This behavior will be discussed later in the paper in relation to the presence of lithium and hydrogen in the spinel structure, shown by chemical and TGA analysis.

Concerning the $LiCoO_2$ phase, the refinement confirms the presence of a large amount of this phase in the case of Co_3O_4(ternary), estimating the amount at 19 wt %. In the case of Co_3O_4 (2.5 M LiOH), a negligible amount of $LiCoO_2$ phase was detected. This phase, when observed, has a c_{hex} parameter of 14.036 Å (Table 2), which is close to the value observed for $LiCoO_2$, with a stoichiometry of one.[31] This excludes the possibility of the presence of Li_xCoO_2 with $x < 0.94$ that could have been obtained in the oxidizing synthesis conditions. For $0.75 < x < 0.94$, the Li_xCoO_2 system is indeed biphasic and contains a mixture of $Li_{0.94}CoO_2$ and $Li_{0.75}CoO_2$; the latter exhibits a c_{hex} parameter of 14.19 Å.[31] Moreover, the *c*/*a* ratio deduced from the refinement is equal to 4.98 for X-ray and 4.99 for neutron, thus being coherent in both cases with the hypothesis of the HT−$LiCoO_2$ form.[31] The cubic LT-$LiCoO_2$ phase exhibits indeed a *c*/*a* ratio equal to 4.90.[25]

Chemical Analysis. Table 3 presents the weight percentages of Co, Li, Na, K, and H determined for the various samples. No significant amount of C or N was detected and the amounts of Na and K were very low. The chemical compositions of Co_3O_4, $LiCoO_2$, and a theoretical spinel phase containing cobalt deficiencies with formula $Co_{2.6}O_4$ are presented as references. The values of the oxidation state of cobalt, obtained by iodometric titration (see the Experimental Section), have also been reported.

In all the samples, the Co content is lower than that in Co_3O_4, which is in good agreement with both hypotheses: either cobalt vacancies or presence of an additional $LiCoO_2$ phase. The composition resulting from the presence of only cobalt vacancies in a spinel structure would stay in the range $Co_{2.4}O_4$−$Co_{2.7}O_4$.

A significant content of lithium was measured in both Co_3O_4 (2.5 M LiOH) and Co_3O_4 (ternary). In the case of Co_3O_4 (2.5 M LiOH), the negligible amount of $LiCoO_2$ detected (0% by X-ray diffraction refinement or 0.5% by neutron refinement) suggests that titrated lithium within the sample may be located in spinel cobalt vacancies, as many authors have reported for similar phases prepared by the high-temperature synthesis method.[20,22−24] In the case of Co_3O_4 (ternary), major part of chemically titrated lithium (1.3 wt %) is related to the presence of an additional $LiCoO_2$ phase together with Co_3O_4, as shown by X-ray or neutron diffraction (around 19% $LiCoO_2$ in Table 2).

Elementary organic microanalysis evidenced significant hydrogen content in the samples. Even if the weight ratio is as low as 0.3%, the resulting H/Co ratio is close to 0.25 and almost independent from the electrolyte used. Hydrogen probably results from the aqueous preparation method. It can be considered in the structure in the form of hydroxyl groups, molecular water, or adsorbed water. Moreover, in biphasic samples, hydrogen can be in one or both phases. In each case, it has to be taken into account to check the phase electroneutrality.

The presence of Co^{4+} in the Co_3O_4(2.5 M LiOH) spinel phase is suggested by the average cobalt oxidation state (determined by iodometric titration) which is higher than in ideal Co_3O_4 spinel (2.72 against 2.66). On the contrary, in the Co_3O_4 (8 M KOH) spinel phase, the cobalt oxidation state was found to be equal to 2.68, which suggests the absence of Co^{4+} ions in this material. As far as Co_3O_4-(ternary) is concerned (biphasic mixture of spinel type

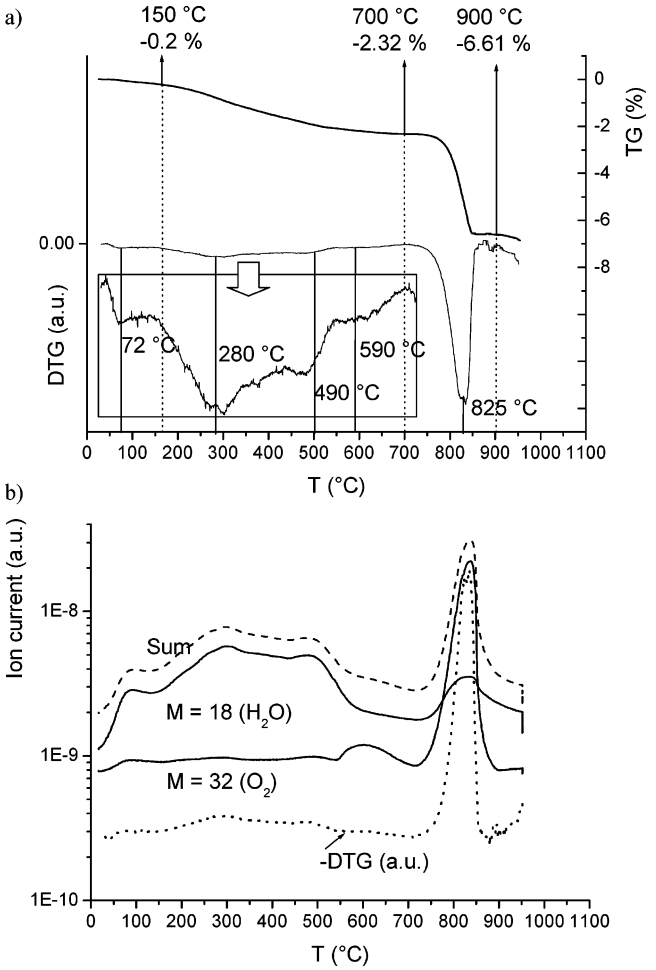

Figure 5. (a) TGA curve and derivative curve and (b) coupled mass spectroscopy curve of Co_3O_4 (ternary). A zoom of derivative mass loss between ambient and 700 °C is displayed, corresponding to the temperature range of the H_2O release. With mass spectroscopy curves, the sum of all released species is also displayed.

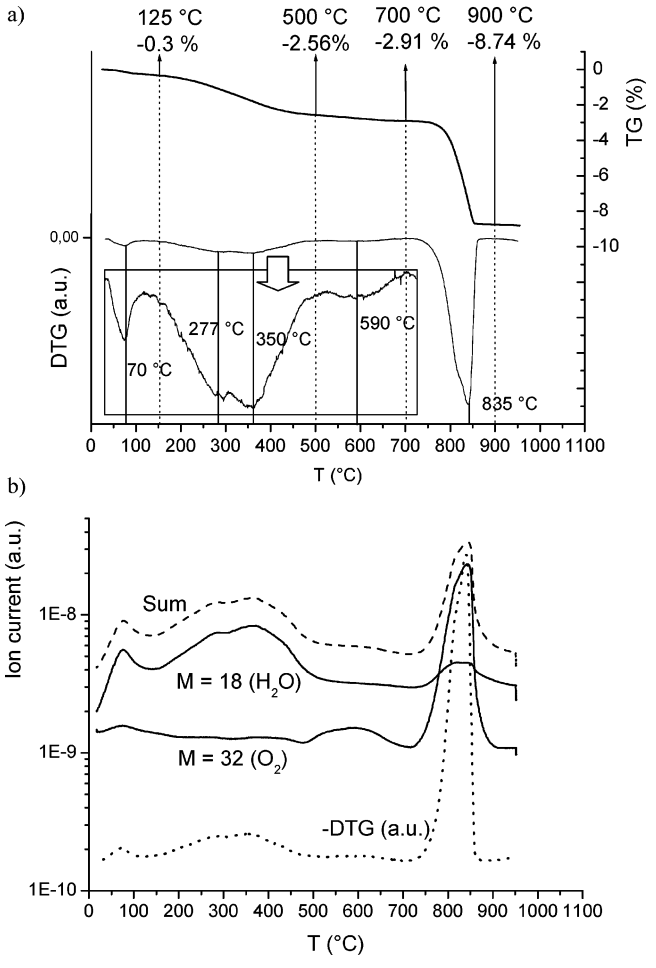

Figure 6. (a) TGA curve and derivative curve and (b) coupled mass spectroscopy curve of Co_3O_4 (2.5 M LiOH). A zoom of derivative mass loss between ambient and 700 °C is displayed, corresponding to the temperature range of the H_2O release. With mass spectroscopy curves, the sum of all released species is also displayed.

"Co_3O_4" phase and $LiCoO_2$), the experimental cobalt oxidation state (2.75) may result from the contribution of Co^{4+} in the spinel phase and of Co^{3+} in $LiCoO_2$.

Thermogravimetric Analysis. In order to get more precise information about the chemical composition of the various "Co_3O_4" phases, a thermogravimetric analysis (under an argon flux) coupled with mass spectroscopy was performed for the samples as described in the Experimental Section. Figures 5−7 present the TGA curves and derivatives curves (DTG) (Figure 5a, 6a, and 7a) as well as the mass spectroscopy (MS) curves of the main released species (Figures 5b, 6b, and 7b) for the three previously studied samples.

The thermal behaviors of the three materials appear to be rather similar. Weight loss curves can be divided into three main parts.

Below 150 °C, a small weight loss can be ascribed to adsorbed water release. It never concerns more than 0.3% initial sample weight.

Between 150 and 700 °C, a significant weight loss is observed for all samples. Actually, it can be divided into several processes, as shown by the derivative curve. All of them correspond to water release, as shown by mass spectroscopy. In this temperature range, water release can be explained only by decomposition of hydroxyl groups. The total weight loss, 2.3−2.9% between room temperature and 700 °C, is also approximately coherent with hydrogen content measured for chemical analysis; 2.3−2.9% water corresponds indeed to 0.26−0.32% hydrogen, which is in good agreement with the values reported in Table 3. The shapes of the derivatives curves are very similar for the material obtained in ternary electrolyte and in 2.5 M LiOH. On the contrary, that of the material obtained in 8 M KOH is very different. At this time, all the detailed differences between the samples have not been explained. But the existence of separated peaks for H_2O release suggests the existence of different hydrogen sites in the structure. Several hypotheses can be envisaged and are currently checked by proton NMR. Protons may be bound to cobalt ions as hydroxyl groups that would be adjacent to octahedral vacancies (16d sites), as observed by Ammundsen et al. in H-exchanged $Li_{1+x}Mn_{1-x}O_4$ spinels,[33] or that could point toward vacant tetrahedral sites (8a site). Water molecules, exhibiting the C_{4v} symmetry, may also be present in vacant tetrahedral sites.

For temperatures higher than 700 °C, the principal weight loss corresponds to the Co_3O_4-to-CoO transition, expected

(33) Aitchison, P.; Ammundsen, B.; Rozière, J.; Burns, G.R.; Jones, D.J. *Solid State Ionics* **2005**, *176*, 813.

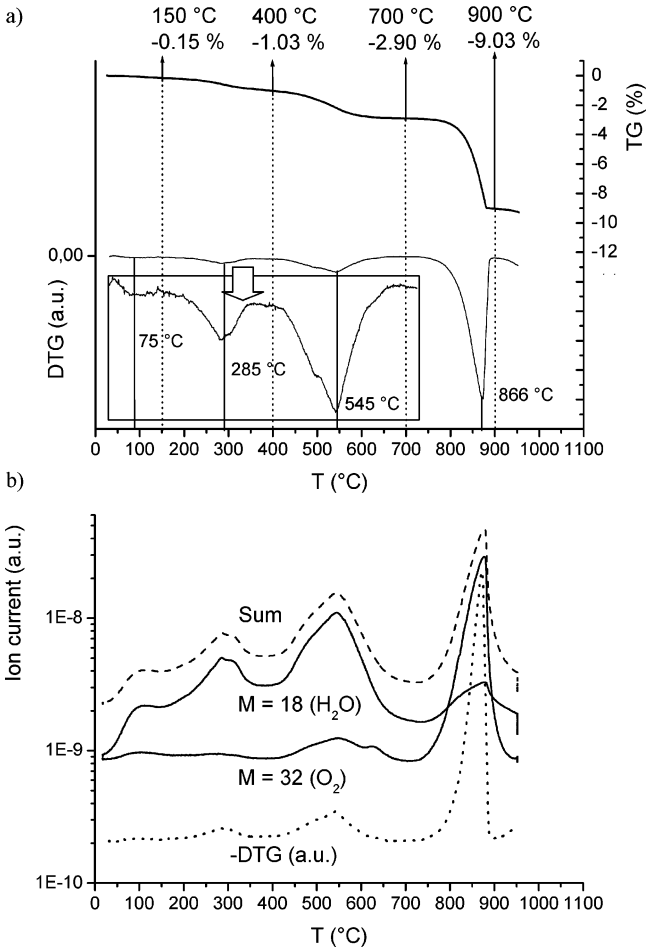

Figure 7. (a) TGA curve and derivative curve and (b) coupled mass spectroscopy curve of Co_3O_4 (8 M KOH). A zoom of derivative mass loss between ambient and 700 °C is displayed, corresponding to the temperature range of the H_2O release. With mass spectroscopy curves, the sum of all released species is also displayed.

under a reducing atmosphere such as argon. Such transformation results theoretically in a 5.88% weight loss, corresponding to oxygen release. If there are cobalt vacancies in the spinel phase and if the charge compensation results in the presence of Co^{4+} ions, the weight loss is expected to increase with the amount of vacancies. However, measured weight loss percentages are not well-related to the amount of cobalt vacancies deduced from chemical analysis. This result suggests that another charge compensation mechanism occurs, like hydrogen or lithium insertion. The XRD patterns of the materials collected after TGA (not presented) are close to that of CoO but with a smaller cell parameter for Co_3O_4 (ternary) and Co_3O_4 (2.5 M LiOH). Such observation suggests that in these two electrolytes, the final material is probably a lithium-substituted cobalt oxide $Li_xCo_{1-x}O$[34]. In this latter material, part of the cobalt ions are in the trivalent state. The reaction that occurs above 700 °C is therefore likely to lead to a smaller oxygen loss than expected for the decomposition of Co_3O_4 into CoO.

As a conclusion, TGA analysis confirms the presence of hydrogen in the spinel structure in different sites.

Discussion about the Refinement of the Structural Data when Considering Li and H in the Spinel Structure. It is now reasonable to discuss the results of refinement of the structural data when considering lithium and hydrogen in the spinel structure.

The refinement in the case of Co_3O_4 (2.5 M LiOH) is not significantly improved when considering the presence of lithium ions in the tetrahedral sites. Nevertheless, when no lithium is taken into account for the refinement, the cobalt amount seems to be underestimated by neutron diffraction compared with X-ray in tetrahedral sites. This behavior may be explained in the following terms. Actually, in the case of neutron, lithium bond scattering length (−1.9 fm) is opposite to that of cobalt (2.5 fm), so that the contributions of both ions on the same site tend to compensate one each other. In the case of X-ray, the number of electrons carried by lithium (3) is really low compared to that on cobalt (27), and the contributions of both ions are just added. If there are some lithium ions in tetrahedral sites, the refinement of the X-ray diffraction data, without taking it into account, should slightly overestimate the real cobalt occupancy, contrary to the refinement of neutron diffraction data of the same material that should noticeably underestimate it. Hence, the observed underestimation of cobalt occupancy in the tetrahedral site by neutron diffraction compared to X-ray diffraction is consistent with the presence of lithium ions in tetrahedral sites. On the contrary, as X-ray and neutron diffraction data refinements lead to the same cobalt occupancy in octahedral sites (see Table 2), there is probably no significant presence of lithium in such sites.

For hydrogen, as its bond scattering length (−3.74 fm) is also opposite that of cobalt and its number of electrons (1) is also negligible compared to that of cobalt, the same tendencies should be observed. Nevertheless, because of its small size, hydrogen is not likely to be located exactly in the cobalt sites. For example, in $Co(OH)_2$, hydrogen is located in tetrahedral sites, but in a noncentered position at a distance of 0.92 Å from one oxygen (instead of 1.95 Å for the center of the tetrahedron).[35] With the present diffraction information, it has not been possible to locate hydrogen precisely. However, the difference between neutron and XRD refinement results should be partly due to its presence, especially in the case of Co_3O_4 (8 M KOH), in which there is no lithium.

Besides, the cell parameter decreases with the amount of vacancies in the tetrahedral site (Table 2). This decrease from Co_3O_4 (8 M KOH) to Co_3O_4 (ternary) and Co_3O_4 (2.5 M LiOH) has to be adressed. In spinel, cell parameter is usually constrained by the size of octahedral sites. If lithium, with its bigger ionic radius than Co^{3+} (0.74 Å for Li^+ and 0.52 Å for Co^{3+}) and its lower charge, was located in octahedral sites, an increase in the cell parameter would be expected; hence lithium is likely to be located in tetrahedral sites, as forecast regarding the occupancies of the cobalt sites. Moreover, the presence of some tetravalent cobalt in octahedral sites, to compensate the positive charge deficiencies due to cobalt vacancies or substitution by lithium and hydrogen, could explain the decrease in the cell parameter.

(34) Johnston, W. D.; Heikes, R. R.; Sestrich, D. *J. Phys. Chem. Solids* **1958**, *7*, 1.
(35) Mockenhaupt, C.; Zeiske, T.; Lutz, H. D. *J. Mol. Struct.* **1998**, *443*, 191−196.

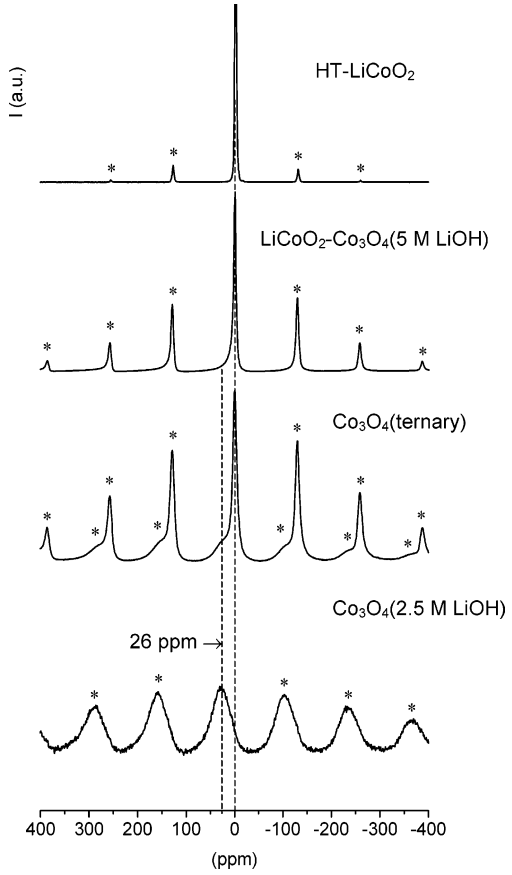

Figure 8. ^{7}Li MAS NMR spectra for the lithium-containing samples Co_3O_4 (2.5 M LiOH) and Co_3O_4 (ternary). Spectra of $LiCoO_2-Co_3O_4$ (5 M LiOH), containing a majority $LiCoO_2$ phase, and pure HT−$LiCoO_2$ are displayed as reference. (★ = spinning sidebands)

^{7}Li MAS NMR Study. To more deeply investigate the lithium-containing phases in the studied samples Co_3O_4 (ternary) and Co_3O_4 (2.5 M LiOH), we performed ^{7}Li MAS NMR measurements on both samples. Only the first of these samples was clearly shown by the diffraction data refinement to contain $LiCoO_2$ in addition to spinel type Co_3O_4. Measurements were also performed for the sample $LiCoO_2-Co_3O_4$ (5 M LiOH), which is a mixture mainly constituted of $LiCoO_2$ (XRD pattern shown in Figure 1e).

The ^{7}Li MAS NMR spectra of the three samples are shown in Figure 8. The spectrum of an ideal HT−$LiCoO_2$ phase, already studied in our group, is also displayed as a reference.[32] Two different signals, with their spinning sidebands, are observed in varying proportions in the studied samples: a narrow, intense signal with no chemical shift (0 ppm), and a broad one, less intense, at 26 ppm. The narrow signal is practically the only one for the $LiCoO_2-Co_3O_4$ (5 M LiOH) sample and disappears for Co_3O_4 (2.5 M LiOH), in which diffraction data refinement estimated the amount of the $LiCoO_2$ phase as negligible. In the case of Co_3O_4 (ternary), in which diffraction shows two phases, both signals are present.

We therefore assign the 0 ppm signal to the $LiCoO_2$ phase. $LiCoO_2$ was actually extensively studied by NMR in our laboratory both for the stoichiometric sample and its deintercalated derivatives, and for Li-overstoichiometric samples.[31,32] Normally, stoichiometric $LiCoO_2$ exhibits a ^{7}Li NMR spectrum close to 0 ppm that is characteristic of a quadrupolar interaction due to the nonperfect symmetry of the electromagnetic field gradient around its site. Actually, the signal recorded here at 0 ppm for our materials and assigned to $LiCoO_2$ is much broader (i.e., its spinning sidebands extend with significant intensity over a wider frequency range), and with a shape more characteristic of strong dipolar interactions. We consider that this is due to the close proximity of this $LiCoO_2$ with the Co_3O_4 type compound, which indeed contains electron spins. The latter may thus exert strong dipolar interactions onto the Li nuclei present in the neighboring $LiCoO_2$ material, leading to the observed NMR spectrum (Figure 8). This effect indeed increases from $LiCoO_2-Co_3O_4$ (5 M LiOH) to Co_3O_4 (ternary), with an increasing $Co_3O_4/LiCoO_2$ ratio. A similar effect was observed on the ^{7}Li NMR line shape of Li_2CO_3 when very intimately mixed with the paramagnetic $LiNi_{1-y-z}Co_yAl_zO_2$ positive electrode material of Li-ion batteries.[36] Another conclusion from these spectra is that, being very close to 0 ppm, the narrow signal can only result from $LiCoO_2$ with a Li content higher than 0.94, because, for smaller Li contents, a metallic phase appears with a Knight-shifted ^{7}Li NMR signal (57 ppm).[31] This confirms the results from the diffraction data refinements, that the $LiCoO_2$ type phase observed here is not metallic. But the presence of a Li_xCoO_2 phase ($0.94 < x < 1$), which, though not metallic, already has a high conductivity, cannot be excluded because lithium in octahedra sharing edges with CoO_6 octahedra containing Co^{4+} ions were considered to be not observable by NMR.[31]

As to the 26 ppm signal, clearly correlated to the presence of the spinel phase, it can be assigned to lithium in the latter structure (note that this signal is very slightly present for the $LiCoO_2-Co_3O_4$ (5 M LiOH) sample in Figure 8), as already suggested by diffraction experiments. This signal is clearly outside the chemical shift range for Li^+ and was not observed to shift significantly within a ca. 20 K temperature range (corresponding to different spinning speeds of the rotor). It is furthermore different in width and position from any reported Li_xCoO_2 signal and is quite similar to that observed for $LiMg_xCo_{1-x}O_2$ phases and attributed to a Knight-shift type interaction resulting from the presence of itinerant holes (formally Co^{4+}), inducing a pseudo-metallic behavior at a local scale around Mg^{2+} ions.[37] Such a behavior can be expected in the materials with spinel structure if the observed cobalt vacancies are filled with lithium and the charge deficiency is compensated by formal oxidation of Co^{3+} ions to Co^{4+}, leading to electron (or hole) delocalization. Again, if Co^{4+} ions with no electron delocalization were present, lithium in the edge-sharing octahedra would not be observed by NMR. The electronic conductivity for these phases, discussed in the following part of this paper, also supports this assignment.

^{7}Li MAS NMR measurements confirm that some lithium has entered the spinel structure in both Co_3O_4 (ternary) and Co_3O_4 (2.5 M LiOH), leading to a material with, at least locally, metallic-type behavior.

(36) Ménétrier, M.; Vaysse, C.; Croguennec, L.; Delmas, C.; Jordy, C.; Bonhomme, F.; Biensan, P. *Electrochem. Solid-State Lett.* **2004**, *7* (6), A140.
(37) Levasseur, S.; Ménétrier, M.; Delmas, C. *J. Power Sources* **2002**, *112*, 419−427.

As a general conclusion of this section, considering the results of X-ray structural refinement (amounts of cobalt in tetrahedral and octahedral sites of the spinel structure), as well as the chemical analysis results (H/Co and Li/Co), we can write the chemical formulas of the pure samples as $H^{+}_{0.58}(Li^{+}_{0.18}Co^{2+}_{0.73})_{tet}\,[Co^{3+}_{1.42}Co^{4+}_{0.38}]_{oct}\,O_4$ for Co_3O_4 (2.5 M LiOH) and $H^{+}_{0.69}(Co^{2+}_{0.88})_{tet}\,[Co^{3+}_{1.88}]_{oct}\,O_4$ for Co_3O_4(8 M KOH).

To establish these formulas, we considered the oxygen stoichiometry to be equal to 4 and the amount of Co^{4+} was determined thanks to electroneutrality. Proposing a chemical formula for Co_3O_4 (ternary) would not be reasonable, because this material is clearly biphasic with a significant amount of $LiCoO_2$. The values of cobalt oxidation state calculated for the above formulas are equal to 2.86 for Co_3O_4 (2.5 M LiOH) and 2.68 for Co_3O_4 (8 M KOH). The latter value is in full accordance with the value determined by titration (Table 3). In the case of Co_3O_4 (2.5 M LiOH), the calculated value is slightly higher than the titrated one (2.72). This difference may be due to the fact that the chemical formula was established in the hypothesis of perfect oxygen stoichiometry. An oxygen stoichiometry lower than 4 could indeed explain the overestimation of the cobalt oxidation state.

4. Electrical Properties

Structural characterization has led to identifying two types of synthesized phases depending on the electrolyte. A Co_3O_4 type phase with cobalt vacancies and hydrogen in the structure is mainly formed in the various electrolytes. Moreover, the amount of cobalt vacancies depends on the electrolyte, and some lithium also enters the structure as soon as LiOH is a component of the electrolyte. In ternary electrolyte, a $LiCoO_2$ type phase is also sometimes formed. Preliminary studies have established a relationship between the presence of lithium in the electrolyte and a good conductivity. We have demonstrated that lithium can be present in the $LiCoO_2$ and non-stoichiometric Co_3O_4 type phases. Electric measurements will thus focus on determining which of these phases plays the key role in the conductivity. In the case of $LiCoO_2$, the presence of a highly deintercalated phase has already been excluded by NMR and diffraction, but the conductivity of Li_xCoO_2 ($0.94 < x < 1$) is high enough to explain an increase in the conductivity of the polyphased samples.[31]

Conductivity Measurements. The variations of the conductivity vs reciprocal temperature of the three studied phases are displayed in Figure 9 with the curve for the reference Co_3O_4 sample presented in the experimental part (XRD pattern, Figure 1a). The values of average activation energy in the range 200−300 K, determined using the Arrhenius formula, are reported in Table 4.

Only materials obtained in lithium-containing electrolytes exhibit high enough conductivity values to be used as conductive additives; the minimum accepted value for industrial applications is indeed around 1×10^{-2} S cm^{-1}. For Co_3O_4 (8 M KOH), the conductivity is close to the value obtained for reference Co_3O_4 and too low to improve the electrode conductivity. The most interesting point is that the sample with the best conductivity and the lower activation energy is Co_3O_4 (2.5 M LiOH). This sample does not contain $LiCoO_2$, as previously shown by NMR and diffraction; therefore, the good conductivity can be attributed only to the nonstoichiometric Co_3O_4 type phase.

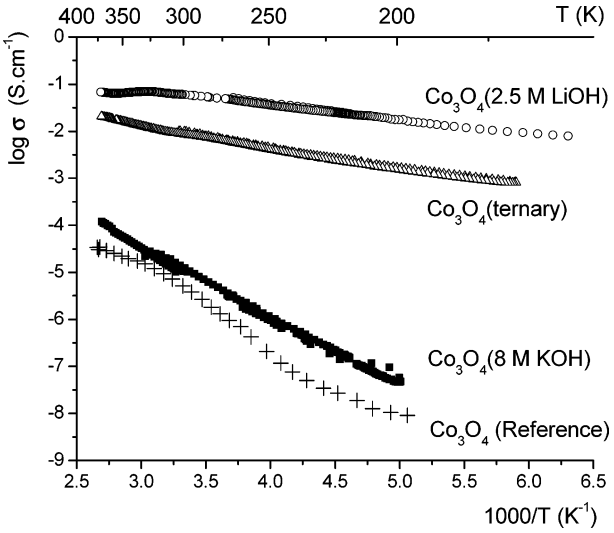

Figure 9. Variation of the logarithm of electrical conductivity vs reciprocal temperature for the studied samples: Co_3O_4 (2.5 M LiOH), Co_3O_4 (ternary) and Co_3O_4 (8 M KOH), in comparison with Co_3O_4 obtained by classical solid-state reaction.

Table 4. Logarithm of the Conductivity at 200 and 300 K and Activation Energy in This Temperature Range for the Studied Samples Co_3O_4 (2.5 M LiOH), Co_3O_4 (ternary), and Co_3O_4 (8 M KOH)

sample	log σ (300 K) (σ in S cm^{-1})	log σ (200 K) (σ in S cm^{-1})	E_a (200−300 K) (eV)
Co_3O_4 (ternary)	−2.07	−2.82	0.09
Co_3O_4 (2.5 M LiOH)	−1.22	−1.76	0.06
Co_3O_4 (8 M KOH)	−4.91	−7.32	0.29

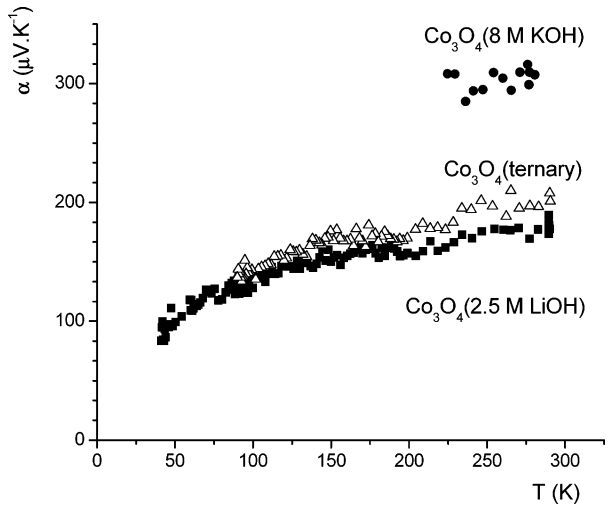

Figure 10. Thermal variation of the Seebeck coefficient for the studied samples: Co_3O_4 (2.5 M LiOH), Co_3O_4 (ternary), and Co_3O_4 (8 M KOH).

All samples show an activated behavior, typical of semiconductors. But the activation energies are low for the most conductive ones. One should also consider the fact that the pellets could not be sintered for conductivity measurements, because of the thermal unstability of the materials. This is likely to lead to grain boundary resistance effects, which must increase the measured resistance and activation

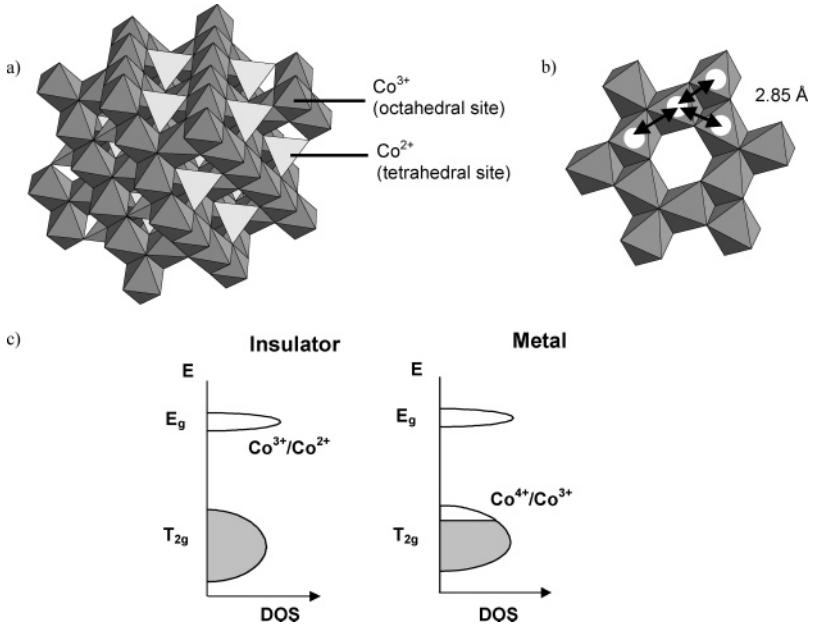

Figure 11. (a) Schematic representation of the spinel structure of the Co_3O_4 phase. (b) Partial representation of the Co^{3+} octahedral sites subnetwork. This environment exists in the three dimensions. (c) Schematic energy diagram of Co_3O_4 illustrating the possible insulator-metallic transition when Co^{4+} ions are created in the octahedral subnetwork.

energy.[38] More information about the conduction mechanism is given by Seebeck measurements.

Thermoelectric Measurements. The variations of the thermoelectric power vs temperature of the studied phases are displayed in Figure 10. Positive values for thermoelectric power mean that, in all cases, majority charge carriers are holes. The shapes of the curves are neither linear, as expected for metallic behavior, nor hyperbolic, like a classical semiconductor with an activated number of charge carriers. Such shape is characteristic of a hopping mechanism, in which the mobility of the carriers is activated with temperature. For Co_3O_4 (8 M KOH), the high resistivity prevented us from recording values at low temperature.

Discussion. This section aims at explaining how a single cobalt spinel as Co_3O_4 (2.5 M LiOH) can exhibit a conducting behavior. As previously described in this paper, Co_3O_4 spinel structure (Figure 11a) can be seen as a three-dimensional subnetwork of Co^{3+} ions in octahedral sites (16d), with Co^{2+} ions in the tetrahedral sites (8a) located at the intersection of the free channels of the octahedral network. The overlapping of the orbitals of the two cobalt sites is not sufficient to allow electronic transfer between the Co^{2+} ions in a tetrahedral environment and the Co^{3+} ions in an octahedral environment. In the octahedral site subnetwork, the distance between adjacent Co^{3+} ions is 2.85 Å (Figure 11b). According to Goodenough's formula,[39] giving critical radius (R_c) for transition elements, R_c is equal to 2.90 Å in the case of Co^{3+} ions. This value is the maximal distance between two atoms allowing electronic delocalization between them. Hence, in our case, it is legitimate to consider a band structure for the octahedral site subnetwork. Then, as presented in Figure 11c for ideal Co_3O_4, the T_{2g} band is full and the E_g band empty. The expected behavior is semiconducting. But as previously explained, some clues, such as a decrease in cell parameters, the NMR signal, or charge balance, suggest strongly the presence of some Co^{4+} in the network. In that case, the T_{2g} band is only partly filled, so that a metallic behavior can be expected. Actually, the conductivity behavior observed corresponds rather to a hopping mechanism. This probably means that the electronic delocalization occurs only at a local scale because of the small Co^{4+}/Co^{3+} ratio and the presence of defects such as Li^+ or H^+ in the structure, with the overall macroscopic conductivity being due to hopping between the metallic zones. This hypothesis allows us to address together the improved conductivity of the material, the Knight-shift type NMR signal, and the hopping mechanism. As mentioned in the NMR section, such behavior was already observed in $LiMg_xCo_{1-x}O_2$ phases, where a pseudo-metallic behavior at a local scale around Mg^{2+} ions was shown.[37]

As a conclusion, the metallic type conductivities are obtained for the Co_3O_4 (2.5 M LiOH) and Co_3O_4 (ternary) materials, which contain Co^{4+} ions in the spinel phase. Moreover, Co_3O_4 (2.5 M LiOH) exhibits the higher conductivity value because it consists of the single metallic spinel phase, whereas Co_3O_4 (ternary) contains a significant amount of $LiCoO_2$, with poorer conductivity.

5. Conclusion

Starting from CoO, by a nonclassical electro-oxidation method in concentrated alkaline electrolytes at 90 °C, various cobalt spinel phases close to Co_3O_4 have been synthesized. In 2.5 M LiOH, a single phase with a spinel structure and a high conductivity has been identified. Its formula is close to $H_{0.60}Li_{0.19}Co_{2.62}O_4$, with cobalt vacancies in both tetrahedral and octahedral sites and lithium and hydrogen in the

(38) Carlier, D.; Saadoune, I.; Ménétrier, M.; Delmas, C.; *J. Electrochem. Soc.* **2002**, *149* (10), A1310.
(39) Goodenough, J. B. *Prog. Solid State Chem.* **1971**, *5*, 278.

structure. At this time, some structural points remain unclear, especially regarding lithium and hydrogen localization. The only partial compensation of the cobalt vacancies by lithium and hydrogen, thus resulting in the formation of Co^{4+} ions in the octahedral sites, leads to the high electronic conductivity of this phase.

Acknowledgment. The authors thank R. Decourt for electric properties measurements, D. Denux for thermogravimetric analysis, M. Basterreix and C. Denage for technical assistance, and SAFT, ANRT, and Région Aquitaine for financial support.

CM060175T